BEAM LOSS AND BACKGROUNDS IN THE CDF AND DØ DETECTORS DUE TO NUCLEAR ELASTIC BEAM-GAS SCATTERING

A.I. Drozhdin, V.A. Lebedev, N.V. Mokhov, L.Y. Nicolas, S.I. Striganov, A.V. Tollestrup
* FNAL, Batavia, IL 60510, USA

Abstract

Detailed simulations were performed on beam loss rates in the vicinity of the Tevatron Collider detectors due to beam-gas nuclear elastic interactions. It turns out that this component can drive the accelerator-related background rates in the CDF and DØ detectors, exceeding those due to outscattering from collimation system, inelastic beam-gas interactions and other processes [1, 2]. Results of realistic simulations with the STRUCT and MARS codes are presented for the interaction region components and the CDF and DØ detectors. It is shown that a steel mask placed upstream of the detectors can reduce the background rates by almost an order of magnitude.

INTRODUCTION

Even in good operational conditions in an accelerator, some particles leave the beam core producing a beam halo. This happens because of beam-gas interactions, intra-beam scattering, proton-antiproton collisions in the interaction regions (IP), and particle diffusion due to RF noise, ground motion and resonances excited by the accelerator magnet nonlinearities and power supplies ripple. As a result of halo interactions with limiting apertures, hadronic and electromagnetic showers are induced in accelerator and detector components causing excessive backgrounds in the detectors. A two-stage collimation system has been developed for the Tevatron Run II [3] to reduce uncontrolled beam losses in the machine to an allowable level. About 0.1% of primary particles hitting the collimators are scattered back into the beam pipe causing collimation system inefficiency. These particles are lost mostly in the high β regions producing the CDF and DØ detectors backgrounds.

The main process of beam-gas interaction, a multiple Coulomb scattering, results in slow diffusion of particles from the beam core causing emittance growth. These particles increase their betatron amplitudes gradually during many turns and are intercepted by collimators. Nuclear elastic beam-gas scattering may increase particle betatron amplitude at one interaction to an amount which exceeds the Tevatron aperture. Many of these particles are lost in the accelerator before they reach collimators located at $5-6\sigma_{x,y}$. It turns out that 25% of them are lost in the vicinity of the IPs adding to the detector background.

A multi-turn particle tracking through the accelerator with elastic beam scattering on the residual gas and halo interactions with the collimators is conducted with the STRUCT code [4]. All the accelerator components with their real strengths and aperture restrictions are taken into account. Using the beam loss distributions calculated this way in the vicinity of the Tevatron's IPs, detailed hadronic and electromagnetic shower simulations with the MARS14 code [5] are performed in the machine, detector and tunnel components. It is found that short steel collimators/masks in the IPs would substantially reduce detector backgrounds induced by nuclear elastic beam-gas scattering.

* drozhdin@fnal.gov

PROTON-NUCLEUS ELASTIC SCATTERING

The products of inelastic interactions of the beam with residual gas nuclei are lost within tens of meters after such interactions. At the same time, scattering angles in nuclear elastic beam-gas interactions are small enough for protons to travel much larger distances in the accelerator and – if not intercepted by collimators – resulting in their loss on limiting apertures. A differential cross section of proton-nucleus (pA) elastic scattering can be parameterized as

$$d\sigma/dq^2 = \sigma_{el}B_{el}e^{-B_{el}q^2} + \sigma_{qel}B_{qel}e^{-B_{qel}q^2}, \quad (1)$$

where $q = p\theta$, p is a proton momentum, θ is a scattering angle, σ_{el} and B_{el} are a total cross section and slope of the coherent pA elastic scattering from the nucleus as a whole, σ_{qel} and B_{qel} are a total cross section and slope of the incoherent pA elastic scattering (scattering which excites or breaks up the nucleus). Total cross sections of these processes are calculated using the Glauber model with inelastic corrections. For a 1-TeV proton on nitrogen, σ_{el} = 115 mb and σ_{qel} = 25 mb. The slope of the coherent scattering is almost independent of energy and can be taken from [6] as $B_{el} = 12.85 * A^{2/3}$ GeV^{-2}. The slope of the incoherent scattering is the same as in the pp elastic scattering: $B_{qel} = 11.0$ GeV^{-2} at 1 TeV. Differential cross section of proton-nitrogen elastic scattering at 1 TeV is shown in Fig. 1 (top) along with a Coulomb scattering contribution calculated from the Rutherford cross section with a Gaussian nuclear form-factor. Note that a total macroscopic cross section of the later process is 8478 cm^2/g, i.e. about 100 times larger than the corresponding elastic cross section. The quality of this formalism is demonstrated in Fig. 1 (bottom) where one can see a good agreement with data [6]. Using the above formulae, one can calculate a probability for proton to scatter elastically on nitrogen to an angle larger than θ_{min} due to strong interactions

$$W_{\theta\geq\theta_{min}} = 0.0011(e^{-11.0q^2_{min}} + 4.6\,e^{-74.5q^2_{min}})\cdot\rho t, \quad (2)$$

where $q^2_{min} = (p\theta_{min})^2$, p is a proton momentum (GeV/c), θ is a scattering angle (radian), ρ and t are a density (g/cm^3) and thickness (cm) of a nitrogen target. Formula (1) was implemented into the STRUCT code for studies of beam-nitrogen elastic scattering described in the rest of this paper with gas pressure given in a nitrogen equivalent.

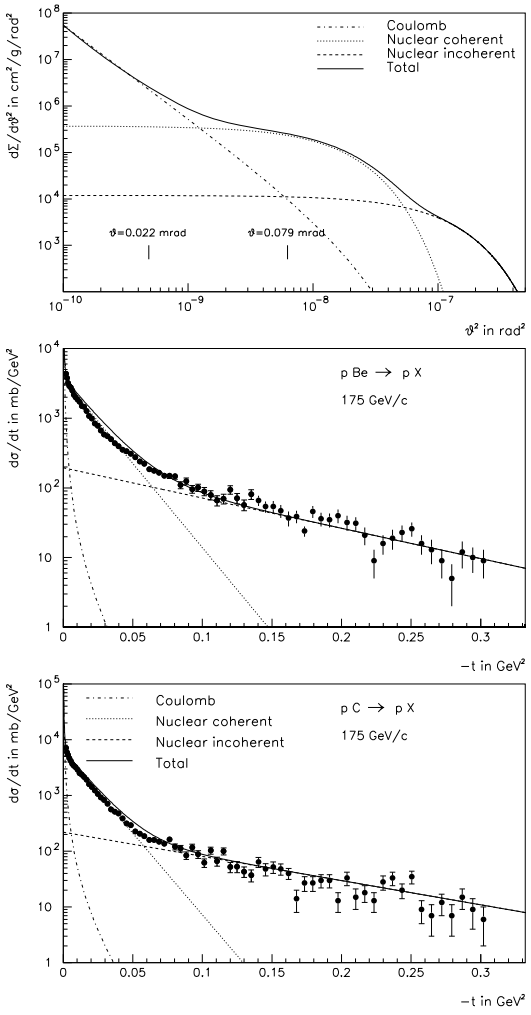

Figure 1: Components of the proton-nitrogen elastic differential cross section at 1 TeV (top) and comparison to experimental data [6] at 175 GeV/c (middle and bottom).

The simulations show that the beam loss rate in the detector regions depends linearly on the gas pressure. Beam loss rate upstream of DØ and BØ as a function of an average gas pressure is shown in Fig. 2. A nuclear elastic beam-gas scattering at a gas pressure $\geq 2\times10^{-10}$ torr exceeds the beam loss in the IPs created by tails from the main collimators. Most of the particles are lost in the separators and in the three dipoles preceding the IPs.

Fig. 3 shows the measured [7] residual gas pressure distribution in the Tevatron Run II along with a calculated beam loss distribution in the ring.

We found that a shadow collimator placed at $13\sigma_x$ ($\pm$11 mm) and $20\sigma_y$ ($\pm$6.3 mm) immediately upstream of the last three dipoles preceding the IPs would allow to suppress the

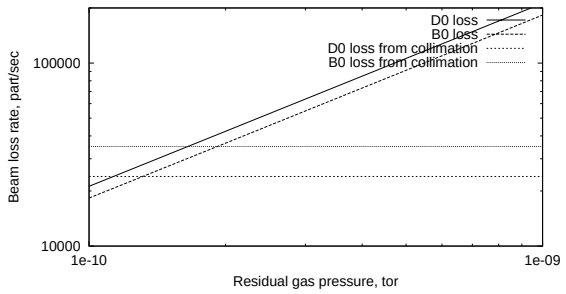

Figure 2: Beam loss rate upstream of DØ and BØ as a function of an average gas pressure. Also shown are beam losses upstream of DØ and BØ originated by the collimation system.

beam-gas induced particle loss in the IPs by an order of magnitude. Details of beam loss distribution in the DØ and BØ regions are shown in Fig. 4 with and without shadow collimator.

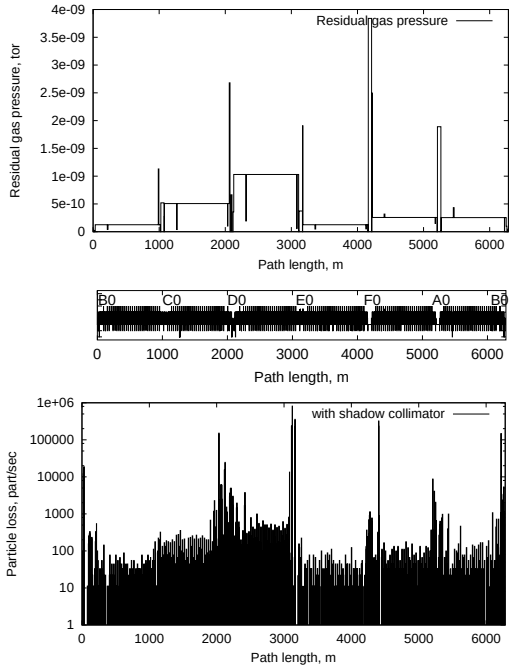

Figure 3: Measured residual gas pressure (top) and beam loss distribution in the Tevatron ring from nuclear elastic beam-gas scattering (bottom).

BEAM LOSS PARTITION

Beam loss rates in the DØ and BØ regions due to nuclear elastic beam-gas scattering and large angle Coulomb scattering – both at the average gas pressure in the ring of 10^{-9} torr – are presented in Table 1 in comparison with those due to elastic $p\overline{p}$ interactions at the two IPs. As shown in Fig. 1 (top), at angles responsible for beam loss in the interaction regions ($\theta \geq 0.079$ mrad), the nuclear elastic scattering cross sections are more than an order of magnitude larger than the Coulomb scattering cross section. As a result, the beam loss rates originated directly from the beam-gas Coulomb scattering and elastic $p\overline{p}$ interactions are two orders of magnitude less compared to the coherent

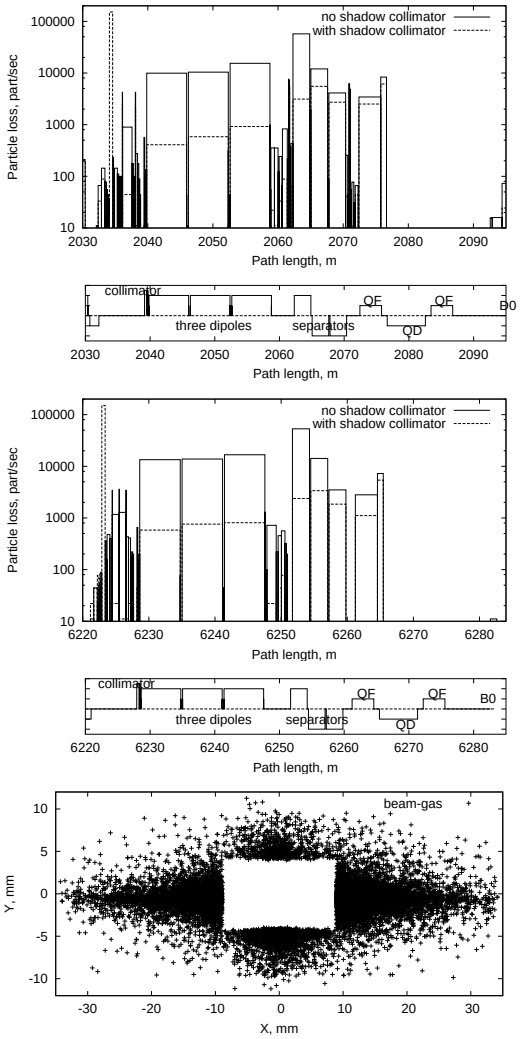

Figure 4: Beam-gas induced loss distributions in the DØ (top) and BØ (middle) regions with and without shadow collimator, and proton hits at the shadow collimator (bottom).

and incoherent beam-gas nuclear scattering.

Table 1: Beam loss rates upstream of DØ and BØ for three sources of particle scattering.

Source	Beam loss rate, s^{-1}	
	DØ	BØ
Nuclear elastic beam-gas	2.04×10^{5}	1.87×10^{5}
Large angle Coulomb beam-gas	2.72×10^{3}	1.40×10^{3}
Elastic $p\overline{p}$ at two IPs	1.44×10^{3}	1.05×10^{3}

BACKGROUNDS IN CDF AND DØ

Fig. 5 (top) shows MARS-calculated charged particle flux in the CDF beam halo monitor (BHM) with and without collimator. The calculations were done with an average pressure of 10^{-10} torr. One sees that the collimator reduces the rates up to one order of magnitude.

The shielding efficiency of a shadow collimator for representative CDF subdetectors is shown in Fig. 5 (bottom) as a function of a distance from the IP for elastic beam-gas scattering as a source. One sees that such a mask reduces

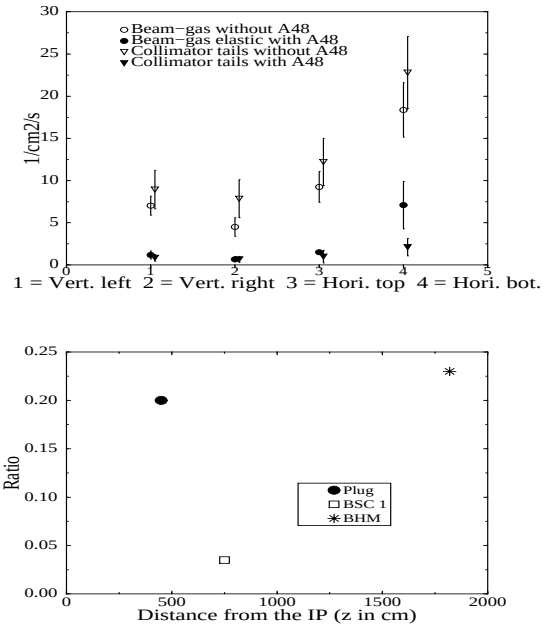

Figure 5: CDF BHM hit rate (top) and the main detector absorbed dose ratio with/without shadow collimator as a function of a distance from the IP (bottom).

the backgrounds in the main detector by a factor of 4.5 to 25. The Beam Shower Counters (BSC) are about a few centimeters to the beam pipe, whereas BHM is at 0.6 m and Plug at 1 m from the beam axis.

CONCLUSIONS

A nuclear elastic beam-gas scattering in the Tevatron generates beam loss in the interaction regions not intercepted by the main collimation system designed for cleaning of slow growing beam halo. This beam loss – and additional background in the DØ and CDF detectors – is proportional to the residual gas pressure. These backgrounds are comparable at an average gas pressure in the machine of about 2×10^{-10} torr to the backgrounds due to tails from the collimation system. A proposed shadow collimators placed in a small phase advance upstream of the last three dipoles preceding the IPs would suppress the beam loss and corresponding backgrounds in the main detectors caused by beam-gas interactions by an order of magnitude.

REFERENCES

[1] A.I. Drozhdin et al. FERMILAB-FN-734, April 2003.

[2] L.Y. Nicolas et al. DØNote-4129, CDF-Note-6407 (2003).

[3] M.D. Church et al. Fermilab-Conf-99/059 (1999).

[4] A.I. Drozhdin et al. "STRUCT Program User's Reference Manual", http://www-ap.fnal.gov/∼drozhdin/

[5] N.V. Mokhov, "The MARS Code System User's Guide", Fermilab-FN-628 (1995); Fermilab-Conf-00/181 (2000); http://www-ap.fnal.gov/MARS/.

[6] A. Schiz et al. *Phys. Rev.*, **D21**, 3010 (1980).

[7] B. Hanna, Residual Gas Pressure Measurements, Aug.02.